Investigation on the Electrostatics Saturation of Flow Electrification in the Liquid Hydrogen Transportation

Bowen Liu, Yanzhong Li *, Lei Wang and Yuan Ma

Institute of Refrigeration and Cryogenic Engineering, Xi'an Jiaotong University, Xi'an 710049, China
* Correspondence: yzli-epe@mail.xjtu.edu.cn; Tel.: +86-29-82668725; Fax: +86-29-82668789

Abstract: Research on the flow electrification characteristic is of paramount importance for ensuring the electrostatic safety of liquid hydrogen transportation systems. However, the discussion about electrostatic saturation in flow electrification has been lacking. To address this gap, a theoretical model governing the process of flow electrification is constructed which couples the charge conservation equation with the Navier-Stokes equations and applies the Neumann boundary conditions at the solid-liquid interface, and the application of this model is validated by existing experimental data with the simulation parameters of A_t and n being 9.08×10^{12} and 0.85 for liquid hydrogen. A comparison with benzene reveals that benzene almost reaches the electrostatic saturation state after flowing one meter, whereas the flow of liquid hydrogen remains in the linear growth stage. However, with an increase in pipe length, a gradual saturation trend emerges in the curves of streaming current versus flow distance when the flow distance exceeds 10 m. At the outlet, the corresponding streaming current and charge density are approximately 160 pA and 3 $\mu C/m^3$, respectively, significantly higher than those observed at one-meter flow distance. Furthermore, the influences of pipe radius and flow velocity on the arrival of electrostatic saturation are analyzed, and the results show that increasing both the pipe radius and flow velocity leads to a delay in the arrival of electrostatic saturation and enhances the saturation value of the streaming current. In conclusion, this study thoroughly discusses the development of flow electrification along with the flow distance and the phenomenon of electrostatic saturation in the long-distance flow of liquid hydrogen, which is crucial for the safe transportation of liquid hydrogen over extended distances.

Keywords: electrostatic saturation; flow electrification; liquid hydrogen; streaming current

1. Introduction

Ensuring electrostatic safety has become a paramount concern in the oil and gas storage and transportation field, leading to increased attention towards flow electrification. The widespread adoption of liquid hydrogen in space propulsion [1], hydrogen energy [2], and other industries calls for a comprehensive assessment of the electrostatic safety of liquid hydrogen transportation systems. Liquid hydrogen possesses explosive properties, characterized by an extremely low minimal ignition energy and a wide explosion range [3,4], making it inherently dangerous. Of particular concern is the accumulation of excess charges generated by flow electrification in storage vessels, leading to the development of high potentials due to the extremely low electrical conductivity of liquid hydrogen [5]. Such high potentials can trigger electrical breakdowns and lead to electrostatic ignitions and explosions.

In our previous studies [6], we extensively researched and analyzed the flow electrification characteristic of liquid hydrogen in pipe flows, focusing on charge distribution and parameter analysis in short pipes of approximately one meter in length. However, it is recognized that the phenomenon of electrostatic saturation in long-distance transportation has received insufficient attention. Understanding electrostatic saturation in long-distance

transportation is crucial for ensuring the safety of liquid hydrogen transportation in various engineering scenarios.

The existence of a double electric layer (EDL) at the solid-liquid interface has been long known [7], comprising the compact layer and the diffusion layer. Numerous theoretical models have been developed to describe the EDL [8]. Flow electrification occurs when excess charges in the diffusion layer migrate into the bulk region, generating an axial streaming current [9]. Research on flow electrification has been conducted for over fifty years, encompassing numerical studies and experimental measurements. Early studies primarily explored steady and fully developed flow electrification issues [10–12], where analytical solutions provided radial distribution of charge density based on certain simplifying assumptions. However, these research efforts failed to address the development of streaming current and charge motion along the flow distance, resulting in a lack of discussion about electrostatic saturation. To address this limitation, Abedian and Sonin [13] introduced a characteristic charge development distance to correct the effect of finite pipe length, leading to an asymptotically saturated streaming current development curve with respect to flow distance. Nonetheless, this model's limited usage is attributed to the challenge of determining charge density at the wall. Providing wall boundary conditions for charge distribution in the form of Dirichlet conditions is unreasonable due to the lack of experimental data. Instead, Neumann conditions are widely employed, connecting current flux at the wall with a chemical reaction rate [10,14]. Theoretically, models using Neumann conditions can also depict the effect of finite pipe length and summarize the electrostatic saturation phenomenon in flow electrification. However, few related works have been performed and reported. In summary, the mechanism of the EDL and the theoretical models of flow electrification have undergone mature development, but electrostatic saturation in flow electrification remains a topic that requires further study.

Experimental research on flow electrification is relatively abundant, and measurements have been conducted even for cryogenic liquids [15,16]. In the case of liquid hydrogen, Cassutt [17] et al. conducted an experimental project to assess the electrostatic hazards associated with the transfer and storage of liquid hydrogen, while Touchard [18] established a test platform to measure the streaming current induced by the pipe flow of liquid hydrogen. However, their focus was primarily on the general evaluation of the intensity of flow electrification, neglecting the variation characteristics along the flow distance and the phenomenon of electrostatic saturation. To study the development of streaming current along the flow distance, Tanka [19] designed an oil circulation pipe system with a four-meter test pipe and installed segmented electrodes on the outer surface of the test pipe to measure leakage currents at different flow distances. The observed curves of leakage current versus flow distance exhibited a downward trend, accurately reflecting the asymptotic saturation of streaming current. While several research studies have explored flow electrification, they typically only measure streaming currents at the outlet or the total output quantity of charges, often neglecting measurements along the pipes. According to Abedian and Sonin's theory [13], it takes around several meters for oils to reach the electrostatic saturation state, implying that the flows of oils are essentially in an electrostatic saturation state in most engineering scenarios. However, the charge development distance for liquid hydrogen can be over tens or hundreds of meters, which renders analysis based on fully developed and steady states of flow electrification unsuitable for most engineering scenarios. Therefore, it is imperative to pay attention to the electrostatic saturation characteristics of flow electrification in the transportation of liquid hydrogen.

In summary, there is a lack of discussion on the electrostatic saturation in flow electrification, especially for cryogenic liquid. In this study, a theoretical model is constructed to govern the process of flow electrification which couples the charge conservation equation and the Navier-Stokes equations and applies the Neumann boundary conditions at the solid-liquid interface, and it is validated using available experimental data with the simulation parameters of A_t and n being 9.08×10^{12} and 0.85 for liquid hydrogen, which is firstly proposed and has a good performance on the prediction of flow electrification

characteristic of liquid hydrogen. The electrostatic saturation of flow electrification is firstly discussed in detail and the development characteristics of flow electrification in liquid hydrogen flows are compared to those in liquid benzene flows to illustrate their differences in electrostatic saturation. Subsequently, the entire process of reaching the electrostatic saturation state for liquid hydrogen is analyzed, followed by a discussion on the influences of pipe radius and flow velocity on electrostatic saturation. This research aims to provide valuable insights into the electrostatic safety of liquid hydrogen transportation, particularly regarding the electrostatic saturation phenomenon.

2. Modeling the Process of Flow Electrification

2.1. Equation of Charge Conservation

In the realm of flow electrification, the fundamental essence lies in the macroscopic manifestation of the governing dynamics that dictate the movement of charged particles, which includes electrons, ions, and charged micro-clusters. These motion patterns arise as a result of the interplay between convection, conduction, and diffusion phenomena. Mathematically, these dynamics can be described by the equation of charge conservation, as shown in Equation (1) [20]:

$$\frac{\partial \rho_q}{\partial t} + \nabla \cdot \mathbf{j} = 0, \tag{1}$$

where ρ_q denotes the charge density, and vector $\mathbf{j}$ represents the current density. In many engineering scenarios involving flow electrification, the systems are in a steady state, allowing us to neglect the first term, $\partial \rho_q / \partial t$, in Equation (1). The second term, which is the divergence of the current density, reflects the spatial distribution of charges and its inhomogeneity. Convection, diffusion, and conduction all contribute to the current density, and their relationship is shown in Equation (2):

$$\mathbf{j} = \underbrace{\rho_q \mathbf{v}}_{\mathbf{j}_{\text{conv}}} - \underbrace{D \nabla \rho_q}_{\mathbf{j}_{\text{diff}}} - \underbrace{\sigma \nabla \phi}_{\mathbf{j}_{\text{cond}}}, \tag{2}$$

where vector $\mathbf{v}$ denotes the fluid velocity, D represents the diffusion coefficient, σ indicates the electrical conductivity of fluid and ϕ signifies the electrical potential. The three contributions induced by convection, diffusion, and conduction are denoted as $\mathbf{j}_{\text{conv}}$, $\mathbf{j}_{\text{diff}}$, and $\mathbf{j}_{\text{cond}}$, respectively. Specifically, $\mathbf{j}_{\text{conv}}$ reflects the influence of the fluid flow field on the motion of charge. The fluid flow field is governed by the continuity equation and the Navier-Stokes equation:

$$\frac{\partial \rho}{\partial t} + \nabla \cdot (\rho \mathbf{v}) = 0, \tag{3}$$

$$\rho \left[\frac{\partial \mathbf{v}}{\partial t} + (\mathbf{v} \cdot \nabla) \mathbf{v} \right] = -\nabla p + \mu \nabla^2 \mathbf{v} + \rho \mathbf{f}, \tag{4}$$

where ρ implies the fluid density, p denotes the pressure, μ represents the dynamic viscosity, and vector $\mathbf{f}$ indicates the external body force. $\mathbf{j}_{\text{diff}}$ is intricately tied to the flow state. In laminar flow conditions, charges primarily undergo diffusion from regions of high concentration to regions of low concentration due to Brownian motion. This diffusion process is characterized by the molecular diffusivity, D_m, which remains constant at approximately 10^{-9} m^2/s. However, in turbulent flow regimes, the dominance of turbulent fluctuations perpendicular to the flow direction supersedes Brownian motion and becomes the principal driving force behind charge diffusion. To accurately describe this augmented effect of turbulent fluctuations on mass diffusion, an additional diffusion coefficient, D_t, is introduced.

In previous studies, the depiction of D_t has often relied on semi-empirical correlations. However, from a fundamental perspective, D_t can be quantified using the turbulent eddy viscosity coefficient, ν_t. This approach provides a more accurate representation of the impact of turbulent fluctuations on charge diffusion in turbulent flow conditions. As for $\mathbf{j}_{\text{cond}}$, it quantifies the influence of the electric field induced by the non-uniform distribution of charges on the behavior of these charges. This non-uniform charge distribution gives

rise to an electric field, which in turn affects the movement and behavior of the charged particles. The relationship between the electric potential (ϕ) and the charge distribution is mathematically established by the Poisson equation, as represented by Equation (5):

$$\nabla^2 \phi = -\frac{\rho_q}{\varepsilon_0 \varepsilon_r},\tag{5}$$

where ε_0 denotes the vacuum dielectric constant, and ε_r implies the relative dielectric constant. Based on the above discussion and incorporating Equations (1), (2) and (5), the charge transport equation can be reformulated as follows:

$$\mathbf{v}\cdot\nabla\rho_q - \nabla\cdot\left[(D_m + D_t)\nabla\rho_q\right] + \frac{\sigma}{\varepsilon_r \varepsilon_0}\rho_q = 0.\tag{6}$$

2.2. Boundary Conditions

In this research article, the main focus is on investigating flow electrification phenomena in a straight cylindrical pipeline used for liquid hydrogen transportation, as depicted in Figure 1. Indeed, the underlying mechanism of flow electrification is an intricate interplay of electrostatic forces and fluid dynamics. This phenomenon can be elucidated by considering the electrical double layers formed at the solid-liquid interface within the pipeline. These double layers consist of a compact layer and a diffusion layer. The excess charges, often represented by positive ions, tend to accumulate within this diffusion layer due to the prevailing electrostatic field effect. When the liquid starts to flow within the pipeline, a compelling sequence of events unfolds. The excess charges present within the diffusion layer experience the combined effects of convection and diffusion, which together propel them into the bulk region of the fluid flow. This migration occurs due to the overlap between the diffusion sublayer and the laminar sublayer, enabling the charges to transition from the confined diffusion layer to the broader fluid volume. As the liquid continues its journey down the pipeline, the excess charges that have been liberated from the diffusion layer now move in synchrony with the bulk fluid flow. This gradual accumulation of charges downstream leads to an evolving distribution of charge density, as visually represented in Figure 1. In essence, the dynamic process of flow electrification can be understood as a result of charges being liberated from the solid-liquid interface, traversing the diffusion sublayer, and eventually being transported along with the fluid flow. This intricate interplay between electrostatic forces, diffusion, and convection underpins the evolution of charge distribution along the flow path, culminating in the phenomenon known as flow electrification.
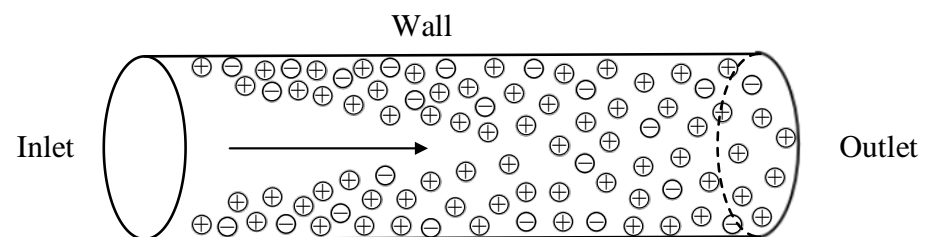
Figure 1. Schematic diagram of liquid hydrogen transport pipelines.

To analyze the flow field within the pipeline, specific boundary conditions are defined for different parts of the system. At the inlet of the pipeline, a velocity inlet boundary condition is specified, where the normal average inflow velocity is denoted as V_a. This condition sets the initial flow velocity of the liquid hydrogen entering the pipeline. The wall surfaces of the pipeline are treated with a no-slip boundary condition. This assumption implies that there is zero relative velocity between the fluid and the walls, signifying that the liquid hydrogen adheres to and moves with the walls of the pipeline. For the outlet of the pipeline, the boundary condition is determined by setting the pressure to the local atmospheric pressure. This condition ensures that the pressure at the exit of the pipeline corresponds to the surrounding atmospheric pressure.

In the context of studying the motion of charges in the fluid, it is assumed that the fluid is electrically neutral. Consequently, the charge density at the inlet of the pipeline is set to zero, as there are no initial charges present. Furthermore, both the fluid flow and flow electrification are assumed to be fully developed. In this scenario, the gradient of charge density at the outlet is set to zero, implying that there is no change in charge density along the flow direction as it reaches the outlet. For the solid-liquid interface, the boundary conditions of charges are given as follows, based on the research by Tanaka [19] and Diao [20]:

$$\left.\frac{\partial \rho_q}{\partial r}\right|_w = c_0 A_t V_a^n, \tag{7}$$

where c_0 denotes the concentration of charges in the fluid under electrically neutral conditions which follow Einstein's relations [21]:

$$c_0 = \frac{\sigma k_B T}{2e_0 F D_m}, \tag{8}$$

where $k_B = 1.38 \times 10^{-23}$ J/K, $e_0 = 1.60 \times 10^{-19}$ C, and F = 96,485.34 C/mol denote the Boltzmann constant, the elementary charge, and the Faraday constant, respectively, and T represents the fluid temperature. The empirical coefficients A_t and n are determined by experimental data.

2.3. Simulation Settings

The numerical simulations in this research article are carried out using a coupled computational fluid dynamics (CFD) and equation of charge conservation approach. The simulations are performed using the commercial software COMSOL Multiphysics version 5.6. To simplify the computation complexity, two-dimensional axisymmetric simulation models are adopted. For mesh generation, the mapped node in the COMSOL meshing module is added to create a rectangular structured grid, in which an even distribution of mesh elements in the axis direction and a segmented distribution in the radial direction are set, and a stepped local mesh refinement technique is applied in the diffusion sublayer to enhance accuracy in that region. The total number of elements is 260,000. The meshing process ensures proper resolution of the flow and charge distribution. To couple the fluid flow and charge conservation equations, a custom mathematical equation interface is used. The classical steady convection-diffusion equation is employed to introduce the equation of charge conservation into the coupling interface. For the calculation of the fluid flow field, the *k-ε* model of Reynolds-averaged Navier-Stokes equations (RANS) is applied. This turbulence model provides reasonable approximations for turbulent flows and enables the simulation of the flow behavior in the liquid hydrogen transportation system.

2.4. Model Validation

Measurement experiments to investigate the effect of turbulence on electrokinetic phenomena for benzene were conducted by Rutgers [22], and the obtained experimental data was utilized to validate the model developed in this study. The experimental setup involved adding Zn-di-isopropyl salicylate solutions with varying concentrations and adjusting the pipe radius, leading to six different experimental series. The simulations were performed based on these experimental conditions, and the results are presented in Figure 2a,b. Remarkably, the simulation results align excellently with all six series of experimental data. To provide a more direct and concise comparison of the validation results, a direct comparison between the measured streaming current, $I_{s,\exp}$, and the simulated streaming current, $I_{s,\text{sim}}$, was made, and the relationship between the streaming current and the charge density is shown in Equation (9).

$$I_s = \int_\Omega u \rho_q ds, \tag{9}$$

where u is the axis flow velocity and Ω is the flow area. The comparison is depicted in Figure 3, where all the scatter points closely cluster around the axis of symmetry. The

average deviation between the measured and simulated streaming currents is found to be only 0.45%, with the maximum deviation reaching −3.46%. This high level of agreement between the experimental and simulated data confirms the accuracy and reliability of the developed model in capturing the electro-kinetic phenomena for benzene under turbulent flow conditions.
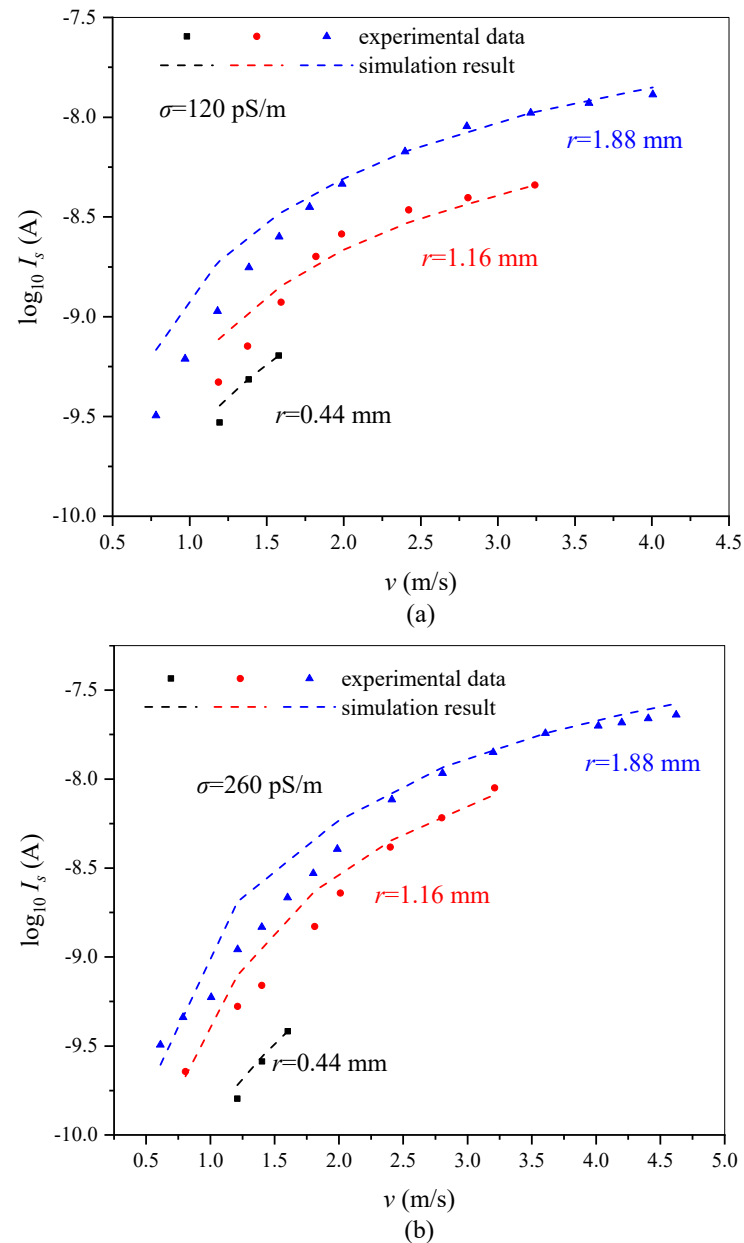
Figure 2. Curves of streaming current versus flow velocity showing a comparison between Rutgers's experiments [22] and our simulations. All the pipes are one meter in length, and the electrical cnductivities of figure (**a**,**b**) are 120 and 260 pS/m, respectively.

It is worth noting that during the validations for benzene, the empirical coefficients A_t and n are set to be 8.94×10^{10} and 0.85, respectively. However, for the simulations of liquid hydrogen, some necessary adjustments are made to these settings. Based on valuable experimental data provided by Touchard [16], average charge density values at the pipe outlet are obtained, and the model was validated using these experimental results. For these liquid hydrogen simulations, the values of A_t and n are adjusted to 9.08×10^{12} and 0.85, respectively. The results of these validations are shown in Figure 4, and it is evident that the simulation results are in the same order of magnitude as the experimental results,

with a generally consistent trend of variation. Considering potential external interference and experimental fluctuations in low-level measurements, it can be concluded that the constructed model and related settings are valid for conducting numerical research on the flow electrification of liquid hydrogen. This validation process ensures the reliability and accuracy of the model in capturing the electro-kinetic phenomena specific to liquid hydrogen flows.
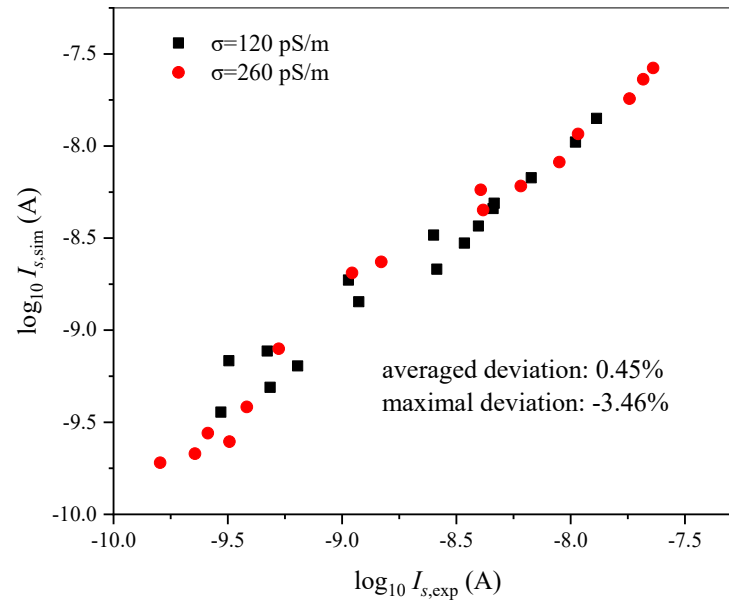
Figure 3. Comparisons between the experimental results [22] and the simulation results.
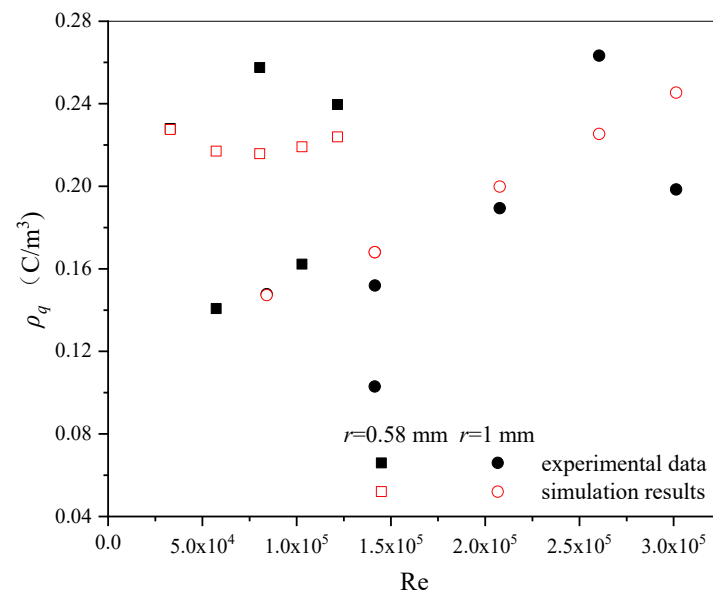
Figure 4. The charge densities of liquid hydrogen flows in different Reynold numbers with a comparison between Touchard's experiments [16] and our simulations.

3. Results and Discussion

3.1. Comparisons between Benzene and Liquid Hydrogen

In the model validation section, comparisons between benzene and liquid hydrogen as fluid media have been performed in detail. Two simulated cases, one for benzene based on Rutgers's experiments and another for liquid hydrogen based on Touchard's experiments [16], are displayed in Figure 5, and the electrical and thermal properties of benzene

and liquid hydrogen used in the simulations are listed in Table 1. To ensure a fair comparison, the averaged fluid velocities, V_a, in these two cases are similar, with values of 4.01 m/s and 5.42 m/s, respectively. Despite differences in numerical magnitude, it is evident that there are significant variations in the trend between benzene and liquid hydrogen. For the benzene case, both the streaming current and the average charge density curves appear to slow and tend to reach a saturation value within a one-meter flow distance, as shown in Figure 5a. This saturation phenomenon has been previously observed and discussed in Abedian's [13] research. However, the curves for liquid hydrogen in Figure 5b show a nearly linear growth, indicating that a one-meter flow distance is insufficient for liquid hydrogen to reach a saturation state, if such a state exists. These distinct differences in the behavior of benzene and liquid hydrogen in flow electrification highlight the importance of considering the specific characteristics of each fluid when assessing electrostatic safety. The observations suggest that the electrostatic saturation state may be reached more quickly in benzene compared to liquid hydrogen. Therefore, it is essential to conduct further investigations and simulations for liquid hydrogen at longer flow distances to better understand its flow electrification behavior and the potential electrostatic hazards associated with its transportation.
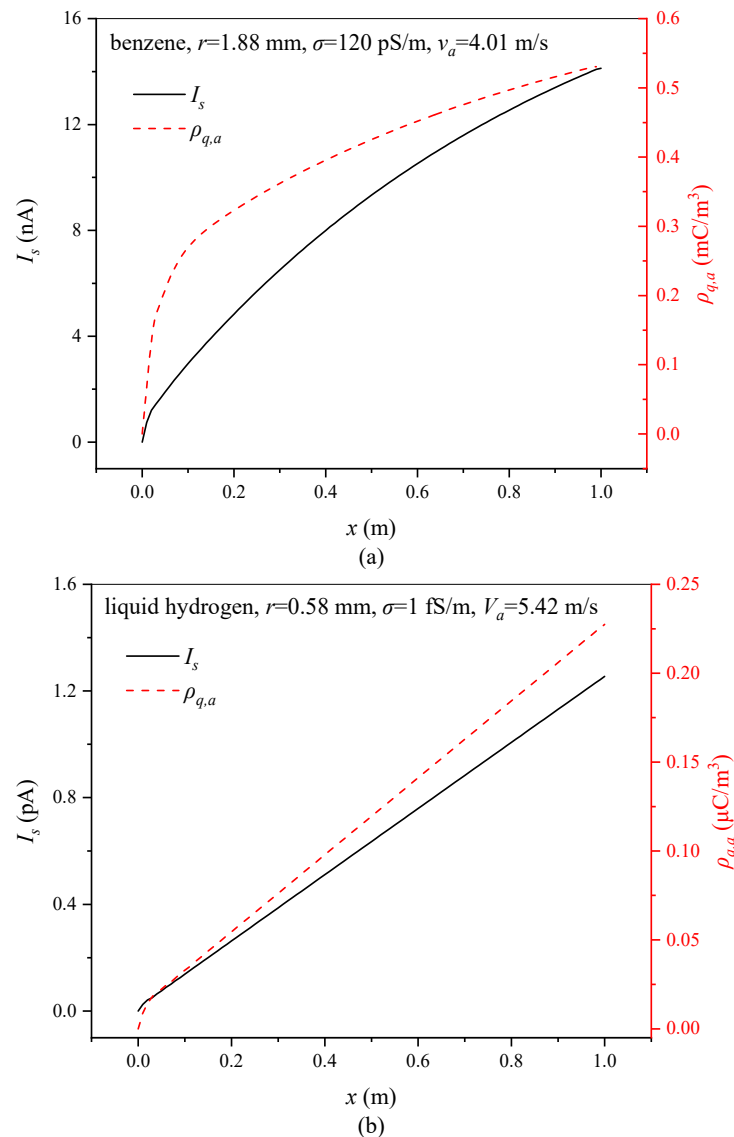
Figure 5. The curves of streaming current and averaged charge density versus flow distance: (**a**) is for benzene and (**b**) is for liquid hydrogen.

Table 1. The electrical and thermal properties of benzene and liquid hydrogen.

Property	Values for Benzene [22]	Values For Liquid Hydrogen [6]
Temperature, T (K)	300.000	20.324
Density, ρ (kg·m^{-3})	871.000	70.899
Relative permittivity, ε_r	3.000	1.231
Electric conductivity, σ (S·m^{-1})	1.200×10^{-10}	1.000×10^{-15}
Molecular diffusivity, D_m (m^2·s^{-1})	1.000×10^{-9}	1.206×10^{-9}
Kinematic viscosity, ν (m^2·s^{-1})	5.000×10^{-7}	1.910×10^{-7}

3.2. Electrostatic Saturation of Flow Electrification in Liquid Hydrogen Transportation

Theoretical analysis suggests that as the flow progresses downstream, charges accumulate, and the inhibitory effect of the conduction term becomes more pronounced. Consequently, there will be a saturation value for the flow electrification of liquid hydrogen transportation. To capture the entire process of flow electrification in liquid hydrogen transportation, including both the initial growth stage and the later saturation stage, the pipe length of the simulated case in Figure 5b has been extended to 30 m while keeping other settings the same. The contours of charge density and flow velocity are displayed in Figure 6, with the radial magnification set to 5000 times for better visualization. In Figure 6, it is evident that the charge density increases along the flow distance. When the flow distance reaches approximately 20 m, the growth rate starts to slow down, and the charge density appears to approach a saturation value. Meanwhile, the flow velocity field appears steady and almost remains in the fully developed stage over very short flowing distances. These results indicate that in the case of liquid hydrogen transportation, there is a transition from the initial growth stage to a saturation stage for flow electrification as the flow progresses. The charge density continues to increase along the flow distance until it approaches a saturation value, while the flow velocity field remains relatively stable. This observation supports the notion that there is a saturation point for flow electrification in liquid hydrogen transportation. However, further investigation and analysis are needed to fully understand the characteristics of this saturation phenomenon and its implications for the electrostatic safety of liquid hydrogen transportation.

The development of the streaming current is a key focus, and its behavior is depicted in Figure 7. The plot shows that the streaming current experiences a nearly linear growth trend in the initial segment of the flow. As the flow progresses downstream, the streaming current gradually approaches a saturation stage. This observation confirms the presence of a saturation phenomenon in the flow electrification process for liquid hydrogen transportation. The evolution process of charge density distribution also provides insights into the saturation of flow electrification. Figure 8 illustrates the radial distribution of charge density at various flow distances. The graph reveals that the charge density is initially high near the surface of the pipe and then rapidly decreases as it approaches the center of the pipe. Moreover, with increasing flow distance, the entire curves of radial charge density distribution shift upwards, indicating an overall rise in charge density. However, the rate of increase becomes smaller, demonstrating the saturation of flow electrification. These findings support the notion that as liquid hydrogen flows through the pipeline, charge density accumulates near the pipe's surface, and the saturation phenomenon leads to a gradual slowdown in the growth rate of both the streaming current and the radial charge density distribution.
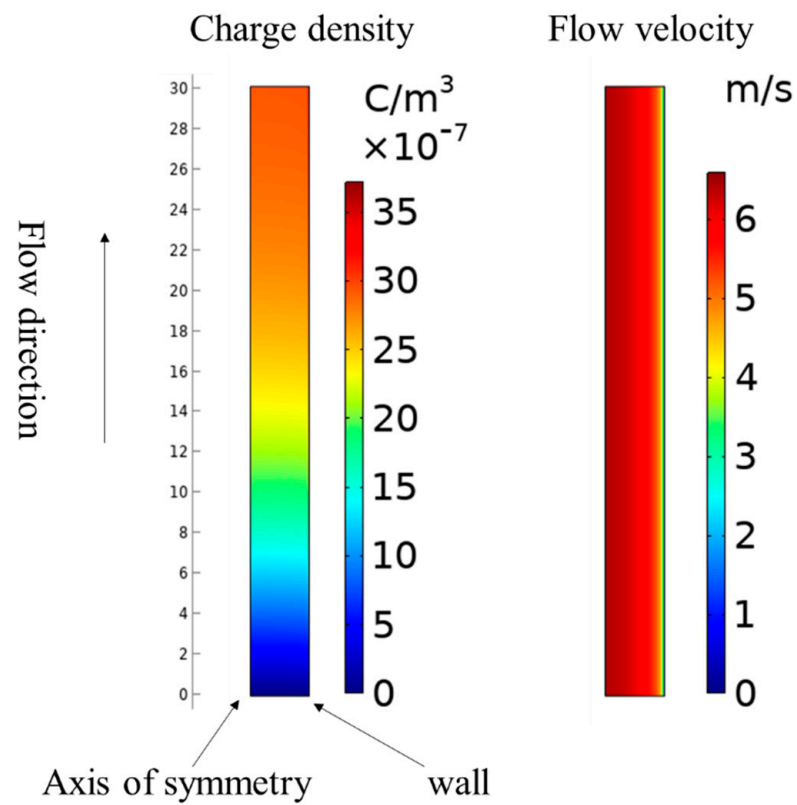
Figure 6. The contours of the distribution of charge density and flow velocity. The radius of the pipe is enlarged by 5000 times in this figure.
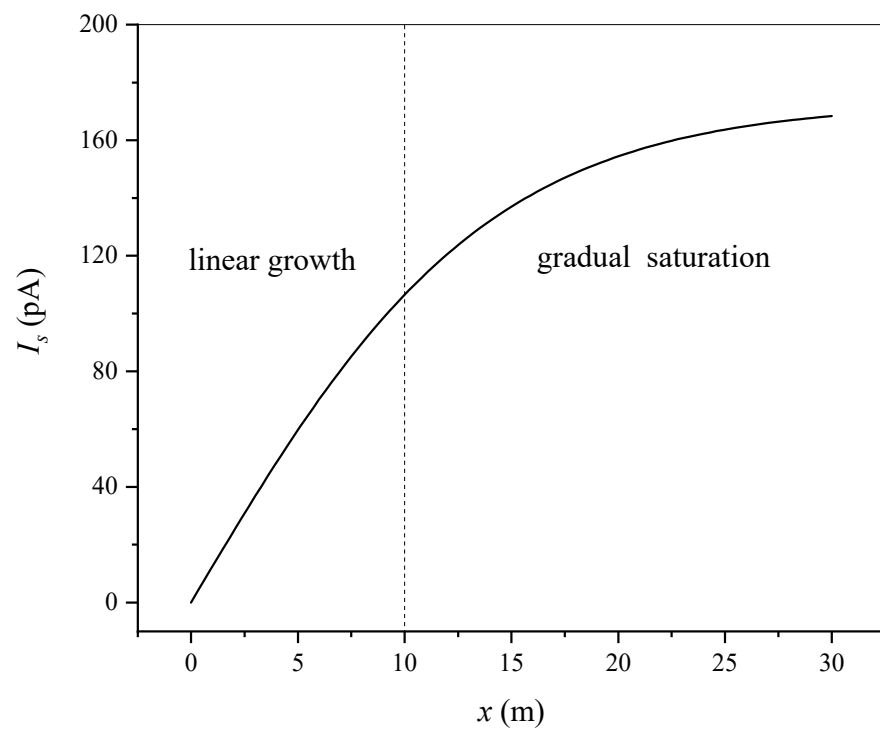
Figure 7. The curve of streaming current versus flow distance of liquid hydrogen.
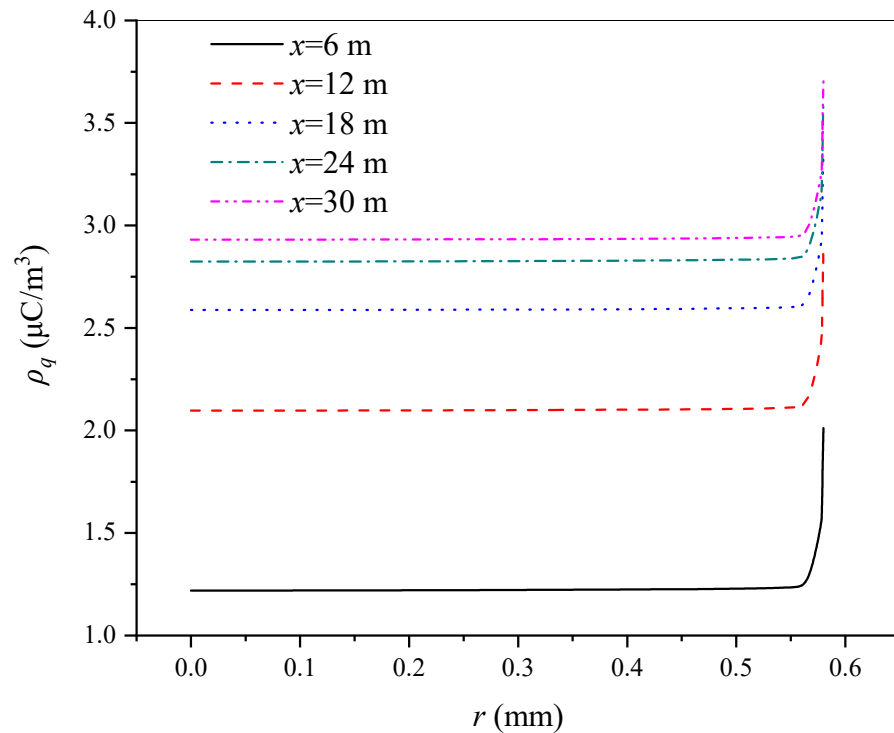
Figure 8. The curves of charge density versus radial coordinate at different flow distances.

3.3. Influences of Pipe Radius and Flow Velocity on Electrostatic Saturation

The results presented above are based on specific condition settings, and it is evident that altering the pipe radius and the flow velocity can have a significant impact on the development process of flow electrification. Figure 9 displays the curves of streaming current versus flow distance with different pipe radii. The flow velocity is kept constant, matching that of the case shown in Figure 6, and the flow distance is extended to 50 m, providing sufficient distance for the case with a pipe radius of 0.58 mm to reach the saturation stage. As the pipe radius increases, it appears to take a longer flow distance to reach the saturation stage. When the pipe radius exceeds 5 mm, the entire process seems to remain in the initial linear growth stage. It can be inferred that the saturated streaming current increases with the rise in pipe radius. Additionally, the radial distribution of charge density at the pipe outlet is analyzed for different pipe radii and plotted in Figure 10. The figure shows that although the charge densities at the wall are relatively consistent, the charge densities at the bulk region significantly decrease as the pipe radius increases. This phenomenon can be attributed to the fact that as the pipe radius increases, it becomes more difficult for the excess charges in the diffusion sub-layer to move to the bulk region of the flow. These observations highlight the importance of considering various factors, such as pipe radius and flow velocity, in the analysis of flow electrification for liquid hydrogen transportation.

The influence of flow velocity is also thoroughly analyzed, and the results are depicted in Figure 11. The range of the Reynolds number is from 5000 to 5×10^5, corresponding to flow velocities that increase from 0.24 m/s to 24.87 m/s, effectively covering a wide range of engineering scenarios. From Figure 11, it becomes evident that the entire curves of streaming current versus flow distance show an upward trend with the increase in flow velocity. Furthermore, it can be summarized that as the flow velocity increases, it takes a longer flow distance for the electrostatic saturation state to be reached.
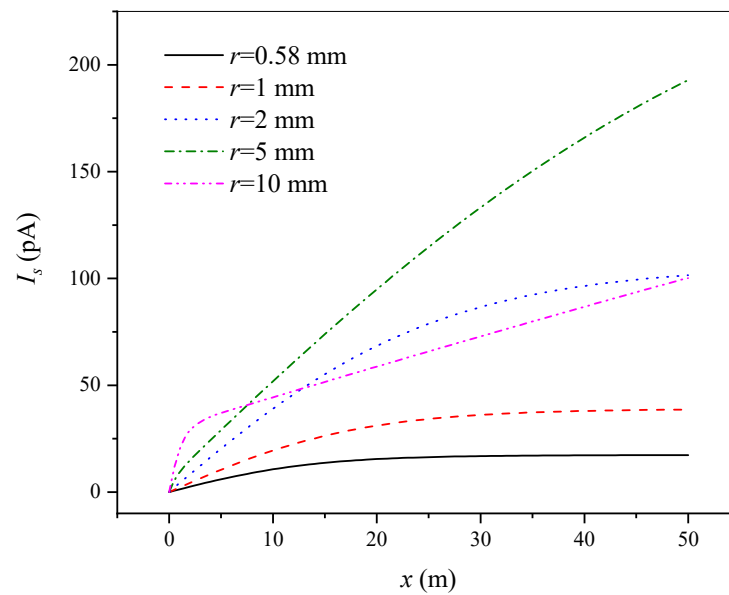
Figure 9. The curves of streaming current versus flow distance with different pipe radii.
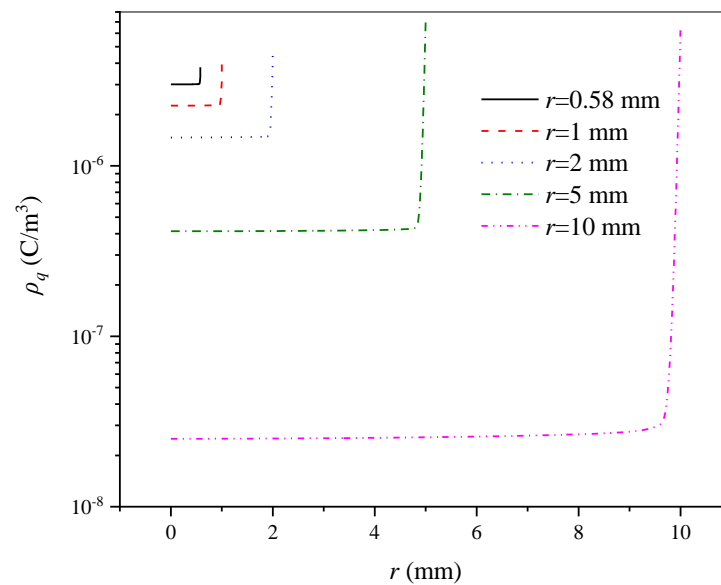
Figure 10. The curves of charge density versus radial coordinate with different radii.

Indeed, the study of electrostatic saturation in liquid hydrogen transportation systems is a multifaceted endeavor that involves considering a range of influencing factors beyond pipe radius and flow velocity. Impurities, encompassing solid particles and gas bubbles, introduce complexity to the electrostatic behavior of the system. These impurities can accelerate the rate of charge generation, potentially leading to an earlier onset of electrostatic saturation. A comprehensive understanding of how impurities interact with the flow electrification process is crucial for accurate safety assessments. Furthermore, the type of liquid being transported also significantly impacts the electrostatic behavior. It involves a comprehensive consideration of parameters such as electrical conductivity, permittivity, density, and viscosity. Each of these factors contributes to the overall electrostatic characteristics of the system. Therefore, a more detailed and nuanced analysis is required to account for the specific working conditions and the interplay of these parameters. Such insights will be pivotal in refining safety measures and operational guidelines for liquid hydrogen transportation systems, ultimately ensuring their robust and secure operation.
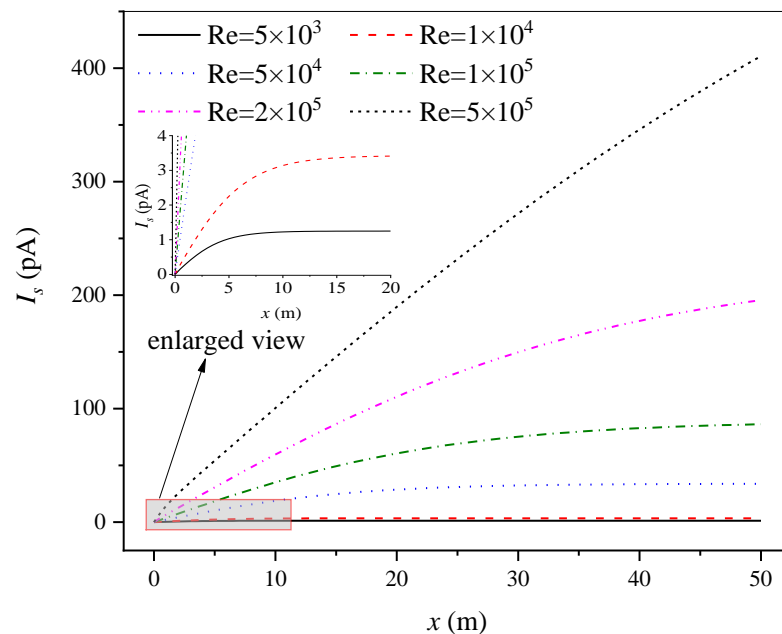
Figure 11. The curves of streaming current versus different Reynold numbers.

4. Conclusions

In conclusion, the research presented in this work focused on the flow electrification of liquid hydrogen and explored the electrostatic saturation characteristic in depth. The key findings and conclusions of this study are as follows:

(1) In the liquid hydrogen flows, flow electrification initially leads to a linear increase in streaming current with the flow distance, followed by a gradual saturation. The distance required for electrostatic saturation in liquid hydrogen is on the order of tens of meters, while for benzene, it occurs within just one meter.

(2) The pipe radius has a significant impact on the electrostatic saturation process. Increasing the pipe radius delays the onset of electrostatic saturation and enhances the magnitude of the saturated streaming current. However, it also results in a decrease in the charge density.

(3) Flow velocity plays a crucial role in flow electrification. Higher flow velocities lead to a longer distance required to reach electrostatic saturation and also result in higher streaming current values throughout the entire flow electrification process.

References

1.	Galeev, A.G. Review of engineering solutions applicable in tests of liquid rocket engines and propulsion systems employing hydrogen as a fuel and relevant safety assurance aspects. *Int. J. Hydrog. Energy* **2017**, *42*, 25037–25047. [CrossRef]
2.	Lowesmith, B.J.; Hankinson, G.; Chynoweth, S. Safety issues of the liquefaction, storage and transportation of liquid hydrogen: An analysis of incidents and HAZIDS. *Int. J. Hydrog. Energy* **2014**, *39*, 20516–20521. [CrossRef]
3.	Crowl, D.A.; Jo, Y.-D. The hazards and risks of hydrogen. *J. Loss Prev. Process Ind.* **2007**, *20*, 158–164. [CrossRef]
4.	Pritchard, D.K.; Rattigan, W.M. Hazards of Liquid Hydrogen: Position paper: Prepared by the Health and Safety Laboratory for the Health and Safety Executive. January 2010. Available online: https://www.h2knowledgecentre.com/content/policypaper1190 (accessed on 6 April 2023).
5.	Bustin, W.M.; Dukek, W.G. *Electrostatic Hazards in the Petroleum Industry*; Electronic & Electrical Engineering Research Studies, No. 2; Wiley: New York, NY, USA, 1983.
6.	Bowen, L.; Yanzhong, L.; Lei, W. Flow electrification characteristics of liquid hydrogen in pipe flow. *Int. J. Hydrog. Energy* **2023**, *48*, 18526–18539. [CrossRef]
7.	Studien über Electrische Grenzschichten—Helmholtz—1879—Annalen der Physik—Wiley Online Library. Available online: https://onlinelibrary.wiley.com/doi/10.1002/andp.18792430702 (accessed on 20 July 2023).
8.	Schmickler, W. Double layer theory. *J. Solid State Electrochem.* **2020**, *24*, 2175–2176. [CrossRef]
9.	Touchard, G. Flow electrification of liquids. *J. Electrost.* **2001**, *51–52*, 440–447. [CrossRef]
10.	Gavis, J. Transport of electric charge in low dielectric constant fluids. *Chem. Eng. Sci.* **1964**, *19*, 237–252. [CrossRef]
11.	Miaoulis, I.N.; Abedian, B.; Darnahal, M. Theory for electric charging in flow of low-conductivity liquids through screens. *J. Electrost.* **1990**, *25*, 287–294. [CrossRef]
12.	Zmarzly, D. Streaming electrification current model in a round pipe in turbulent regime. *IEEE Trans. Dielectr. Electr. Insul.* **2013**, *20*, 1497–1509. [CrossRef]
13.	Abedian, B.; Sonin, A.A. Theory for electric charging in turbulent pipe flow. *J. Fluid Mech.* **1982**, *120*, 199–217. [CrossRef]
14.	Roach, J.; Templeton, J. An Engineering Model for Streaming Electrification in Power Transformers. In *Electrical Insulating Oils*; Erdman, H., Ed.; ASTM International: West Conshohocken, PA, USA, 1988; pp. 119–135. [CrossRef]
15.	Mizuno, Y.; Okada, H.; Minoda, A. Electrification of liquid nitrogen flowing in electrical insulating pipe. In Proceedings of the 2003 Annual Report Conference on Electrical Insulation and Dielectric Phenomena, Albuquerque, NM, USA, 19–22 October 2003; pp. 229–232. [CrossRef]
16.	Touchard, G. Turbulent flow electrification with hydrocarbon liquids, liquid hydrogen, liquefied natural gas (LNG) and liquid nitrogen: Part II—Experiments and comparison with different models. *Int. J. Plasma Environ. Sci. Technol.* **2021**, *15*, e02013. [CrossRef]
17.	Cassutt, L.; Biron, D.; Vonnegut, B. Electrostatic Hazards Assocated with the Transfer and Storage of Liquid Hydrogen. In *Advances in Cryogenic Engineering*; Timmerhaus, K.D., Ed.; Springer: Boston, MA, USA, 1962; pp. 327–335. [CrossRef]
18.	Touchard, G.; Marcano, L.; Borzeix, J. Streaming currents in flows of cryogenic liquids. In Proceedings of the 1987 9th International Conference on Conduction and Breakdown in Dielectric Liquids, Salford, UK, 27–31 July 1987; pp. 260–265.
19.	Tanaka, T.; Yamada, N.; Yasojima, Y. Characteristics of streaming electrification in pressboard pipe and the influence of an external electric field. *J. Electrost.* **1985**, *17*, 215–234. [CrossRef]
20.	Diao, X.; Jiang, J.; Ni, L.; Mebarki, A.; Shen, G. Electrification hazard of turbulent pipe flow: Theoretical approach and numerical simulation. *Process Saf. Environ. Prot.* **2022**, *159*, 84–95. [CrossRef]
21.	Landsberg, P.T.; Guy, A.G. Activity coefficient and the Einstein relation. *Phys. Rev. B* **1983**, *28*, 1187. [CrossRef]
22.	Rutgers, A.J.; de Smet, M.; de Myer, G. Influence of turbulence upon electrokinetic phenomena. Experimental determination of the thickness of the diffuse part of the double layer. *Trans. Faraday Soc.* **1957**, *53*, 393. [CrossRef]